Materials Science and Engineering B 314 (2025) 118007

Contents lists available at ScienceDirect

Materials Science & Engineering B

journal homepage: www.elsevier.com/locate/mseb

Impact of triiodide ion incorporation on the absorption and photovoltaic efficiency of Bismuth-Based hybrid compounds

César Tablero-Crespo

Instituto de Energía Solar, E.T.S.I. de Telecomunicación, Universidad Politécnica de Madrid, Avenida Complutense 30, 28040 Madrid, Spain

ARTICLE INFO

Keywords:
Solar cells
Optoelectronics properties
Efficiency
Bi-based hybrid compounds

ABSTRACT

To determine whether the incorporation of triiodide ions into Bi-based hybrid compounds can serve as a substitute for iodoplumbates perovskites without diminishing photovoltaic efficiency, we analyzed the contributions of anions and triiodide ions to the absorption coefficients and conversion efficiencies across several compounds, both with and without triiodide ions. The electronic properties and absorption coefficients were obtained from first principles. To determine and quantify the key contributors to the optical gaps, the absorption coefficients and solar cell efficiencies are split as exact many-species expansions. The results reveal that while the triiodide contribution to the absorption coefficients and efficiencies is substantial, the primary distinction between compounds is attributed to the Bi-Bi interatomic distances. Nevertheless, the introduction of triiodide ions results in an increase in efficiency compared to the precursor compounds that lack triiodide ions.

1. Introduction

Organic–inorganic perovskites have attracted great attention for photovoltaic applications due to its high absorption coefficient, and consequently, a high photovoltaic conversion efficiency [1,2]. For example, methylammonium lead iodide $CH_3NH_3PbI_3$ (MAPI) is a widely used iodoplumbate perovskite because of its relatively high-power conversion efficiencies exceeding 23 % and could compete with commercial polycrystalline silicon solar cells. Nevertheless, advances in composition engineering, defect passivation, and device architecture [3–5] have enabled an increase in efficiency to approximately 26 % [3,6,7]. However, the use of iodoplumbates is limited because of lead toxicity and its low stability in ambient conditions. For these reasons, the study of new lead-free semiconducting hybrids with strong light absorption is significant to both scientific research and commercial applications.

Other alternatives using perovskites have been studied, where lead is replaced by other metals with less toxicity. A possibility is exploring compounds containing atoms with an oxidation state of + 2 lead-like. These include elements from the same group in the periodic table, characterized by similar outer shell orbitals. Other examples with an oxidation state of + 2 are Sn and Ge [8–10], alkaline earth metals (Be, Mg [11], Ca [12], Sr [13], and Ba [14]), and other alternatives (V, Mn, Ni, Cd, Hg, Ga, and In [15]). Other possibility is to increase efficiency and stability with inverted perovskite solar cells through suppression of multiple defects [6]. In addition to the nature of cations, anion migration plays a crucial role in the performance and stability of halide perovskite solar cells [16,17]. Specifically, the migration of iodine ions has been extensively analyzed in the literature [16]. Therefore, as we will discuss later, this study will employ compounds with different and more complex crystalline structures than those of halide perovskites.

Although compounds based on the perovskite structure are good absorbers of solar radiation, it is not necessary to have this crystalline structure for alternative candidate compounds [18]. Therefore, other alternative to the iodoplumbate perovskites is the Bismuth-based hybrid organic–inorganic halides [19–26] because of their low toxicity and high stability with respect to the iodoplumbate perovskites. The high stability and environmentally friendly feature make these compounds promising candidates as light-absorbing materials for the photovoltaic and optoelectronic applications. However, the conversion efficiency of the iodobismuthates is still lower than the Pb-based perovskites because the bandgap of iodobismuthates is usually larger than that of iodoplumbates perovskites. A strategy to obtain a narrow bandgap close to that of iodoplumbate perovskites is to incorporate to the Bi-based hybrid perovskites other ions, such as triiodide ion.

Although the optical response of perovskite compounds is indirectly influenced by the organic cation, the primary component affecting their optoelectronic properties is the inorganic anion network [27], i.e. the Pb-I interactions [10] in the PbI_6 octahedra [28]. In any case, to obtain good alternative solar radiation absorbing materials to perovskite-based

E-mail address: cesar.tablero@upm.es.

https://doi.org/10.1016/j.mseb.2025.118007
Received 25 October 2024; Received in revised form 9 January 2025; Accepted 11 January 2025
Available online 16 January 2025

compounds, the absorption coefficients should be similar to those of iodoplumbed perovskites. This also involves having a similar bandgap since it corresponds to the absorption threshold. Therefore, the incorporation of triiodide ions into Bi-based hybrid perovskites could be a strategy to achieve materials with high absorption like those of the iodoplumbate perovskites.

In this work is examined whether iodoplumbate perovskites can be replaced by less toxic Bismuth-Based hybrid compounds without compromising ~~their~~ the solar radiation absorption capacity. The main optical properties are analyzed and compared with existing literature. This information is crucial, as a significant change in the optical properties due to the substitution of Pb with Bi, and the change to more complex crystalline structure, could drastically alter the main parameters of the solar cell. One key property determining the efficiency of solar energy conversion is the absorption coefficient. In this work a theoretical methodology of general interest is employed, where the absorption coefficients and photovoltaic efficiencies are split into contributions through exact many-species expansions. The results of this work allow: (i) To quantify the main contribution to the absorption capacity as a function of photon energy, because the absorption coefficients are decomposed into contributions involving atomic species. (ii) To evaluate the impact of triiodide ion incorporation on the optical energy gap, absorption, and photovoltaic efficiency. (iii) To relate the absorption and solar cell efficiency to the composition and structure. (iv) To assess the potential of substituting lead with other elements to maintain high absorption capacity and reduce toxicity.

One possible strategy is to introduce triiodide ions I_3^- into Bi-based hybrid precursor compounds Z1 and K1, with chemical formulas $(C_6H_{14}N)_3Bi_2I_9$ and $(C_8H_{22}N_2O)Bi_2I_8$ respectively, to obtain the compounds Z2 and K2, with chemical formulas $(C_6H_{14}N)_4(BiI_6{\cdot}I_3)$ and $(C_8H_{22}N_2O)_6(Bi_3I_{14}{\cdot}I_3)_2$ respectively (Table 1). For the growth of Z2 crystals, Z1 was re-dissolved in an oxidized hydroiodic acid solution, and after slow evaporation in a few days Z2 crystals were obtained [29]. Crystals of the K1 and K2 compounds can be grown by solution volatilization at room temperature [30].

The (Z1|Z2) and (K1|K2) experimental bandgaps are (2.02|1.58) eV [29] and (1.91|1.59) eV [30] respectively (Table 2). Therefore, the intercalated triiodide ions have an important role in the electronic and optical properties. In both cases, the insertion of the triiodide ions leads to a reduction of the optical gap with respect to the precursor compounds. This indicate that the intercalated triiodide ion could increase the light absorption capability of the compounds because the Z2 and K2 gaps are close to that of MAPI (~1.5 eV).

In this work we analyze the properties of the precursor compounds Z1 and K1 (without triiodide ions I_3^-), comparing them with those of the compounds Z2 and K2 obtained from the previous precursors by intercalating triiodide ions I_3^-. It's important to note that the composition of these iodobismutates is significantly more intricate than that of halide perovskites. This complexity is evident in the crystalline structures (Table 1). Consequently, the analysis will include both the influence of iodine linkers and the characteristics of the crystalline structures.

In order to analyze the electronic and optical properties, along with their structural origins, first principles calculations will be employed. Furthermore, the optical properties and solar efficiencies will be split into species contributions using exact many-body expansions [27,28].

Table 2
Bandgaps (eV) for the Z1, Z2, K1, K2 compounds obtained experimentally, theoretically, and those obtained in this work.

	Z1	Z2	K1	K2
Experimental	2.02 [29]	1.58 [29]	1.91 [30]	1.59 [30]
Theoretical	2.66 [29]	2.15 [29]	2.51 [30]	2.00 [30]
This work	1.98	1.50	1.90	1.28

This approach allows for the identification and quantification of the most fundamental factors influencing absorption coefficients and solar cell efficiencies, thus linking optoelectronic properties to the structure. Of particular interest is the analysis of the impact of triiodide ions on these properties. Such an analysis is significant because any alteration in optical properties due to structural changes could substantially diminish the efficiency of these materials as solar radiation absorbers. Finally, the results will be compared with experimental data from the literature. From results, the optical properties and solar cell efficiencies are primarily dominated by the anionic fragment of these compounds.

2. Methodology

Electronic structure and optical properties calculations were accomplished using Density Functional Theory (DFT) [31] with periodic boundary conditions and a customized version of the SIESTA code [32]. The exchange–correlation potential was computed employing the Perdew-Burke-Ernzerhof [33] (PBE)functional within the framework of the Generalized Gradient Approximation (GGA). For modeling the inner electron shells, we employed the Troullier–Martins [34] pseudopotentials expressed in the Kleinman–Bylander [35,36] form. Additionally, the outer electron shell states were described using a localized pseudoatomic double-zeta and triple-zeta with polarization orbital basis set [37]. To sample the Brillouin zone of the (Z1|Z2|K1|K2) compounds (60|60|20|18) k-point grids have been used respectively.

The optical properties are obtained using the Kramers-Kronig relationships [38] from the imaginary part of dielectric function. The absorption coefficients are split into species contributions using an exact many-species expansion [27,28]. This expansion arises when the optical transition probabilities, which are proportional to the square of the elements of the momentum matrix, are decomposed into inter-species contributions. With the absorption coefficients divided into species contributions ($\alpha_T = \sum_i \alpha_i$), the total efficiency η_T can also be split as an exact many-species expansions ($\eta_T = \sum_i \eta_i$) [10].

3. Results and discussion

The Z1 compound (Table 1), with chemical formula $(C_6H_{14}N)_3Bi_2I_9$, adopts a zero-dimensional (0D) perovskite-like structure. The anionic structure consists of isolated face-sharing octahedra $[Bi_2I_9]^{3-}$(Fig. 1a). The Z2 semiconductor $(C_6H_{14}N)_4BiI_9$ was obtained by intercalating triiodide ions I_3^- into the Z1 compound. After inserting I_3^- ions, the crystal structure changes notably. The Z2 compound has an anion structure $[BiI_9]^{4-}$. This structure consists of isolated $(BiI_6)^{3-}$ ions separated by triiodide ions I_3^- (Fig. 1b), i.e. $[BiI_9]^{4-} = \left[(BiI_6)^{3-}{\cdot}I_3^-\right]$. In the Figures the iodine atoms have been divided into 3 groups: atoms bonded

Table 1
Main Crystallographic data of the compounds analyzed.

Label	Z1	Z2	K1	K2
Chemical formula	$(C_6H_{14}N)_3Bi_2I_9$	$(C_6H_{14}N)_4(BiI_6{\cdot}I_3)$	$(C_8H_{22}N_2O)Bi_2I_8$	$(C_8H_{22}N_2O)_6(Bi_3I_{14}{\cdot}I_3)_2$
Spacegroup	*Pnma* (n° 62)	$P\bar{1}$(n° 2)	$P2_1/c$ (n° 14)	$P2_1/c$ (n° 14)
Lattice parameters (a|b|c) (Å)	(30.15|8.60|16.12)	(8.53|10.20|14.07)	(10.49|24.89|12.33)	(20.15|22.79|14.99)
Lattice parameters (α|β|γ) (^{0})	(90.00|90.00|90.00)	(91.02|102.75|100.40)	(90.00|113.34|90.00)	(90.00|91.47|90.00)

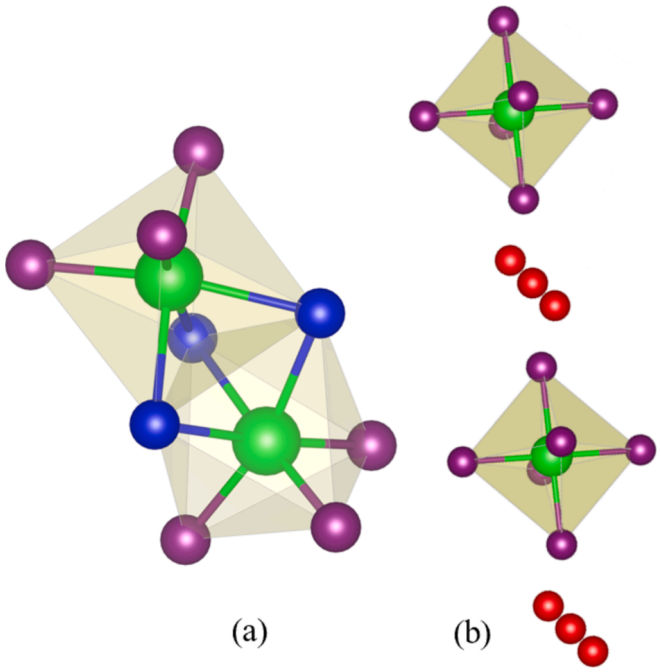

Fig. 1. Crystalline structure of the anionic fragment of the (a) Z1 and (b) Z2 compounds. Atoms are drawn as Bi (green), I (violet, iodine atoms bonded to bismuth), I_l (blue, iodine bridging linkers atoms bonded to two bismuth simultaneously), and I_i (red, iodine atoms not directly bonded to bismuth). (For interpretation of the references to colour in this figure legend, the reader is referred to the web version of this article.)

to a single Bi, bridge linker atoms bonded to two Bi simultaneously (I_l), and atoms not directly bonded to bismuth (I_i). The I_i atoms correspond to the triiodide ion I_3^-, i.e.$I_3^- \equiv (I_i)_3^-$.

The K1 compound (Table 1), with chemical formula $(C_8H_{22}N_2O)Bi_2I_8$, also adopts a 0D perovskite-like structure. The anion part $[Bi_4I_{16}]^{4-}$ (Fig. 2a) is composed of corner-sharing BiI_6 octahedral, in which the central bismuth atom coordinates with six iodine atoms. The crystal K2 was formed after inserting triiodide ions into the K1 compound. The K2 semiconductor has the chemical formula $(C_8H_{22}N_2O)_6Bi_6I_{34}$. The K2 anion structure $[Bi_6I_{34}]^{12-}$ consists of $[Bi_3I_{14}]^{5-}$ and triiodide ion (Fig. 2b), i.e. $[Bi_6I_{34}]^{12-} = 2\left\{[Bi_3I_{14}]^{5-}\cdot I_3^-\right\}$.

The experimental optical gaps for the different compounds, extrapolated from Tauc plots ~~from~~ of absorbance and diffuse reflectance spectra data, and the theoretical results ~~in~~ from the bibliography are shown in Table 2, together with those obtained in this work.

For all the compounds considered, the theoretical optical gaps from this work align well with the experimental results in the literature. According with these results, in Z2 and K2 compounds, the triiodide ion has a significant effect on the electronic properties with respect to Z1 and K1 precursor compounds.

From a study of the projected density of states (PDOS), the valence band (VB) edge states of the Z1 and K1 precursor compounds mainly result from the p(I) states, while the conduction band (CB) states come mainly from the p(Bi) and p(I) states. It indicates that the inorganic Z1 and K1 anion ($[Bi_2I_9]^{3-}$ and $[Bi_2I_8]^{2-}$ respectively) states mainly determine the states close to the band edges. In contrast, the Z2 and K2 electronic structure displays drastic changes with respect to Z1 and K1 compounds after intercalating the triiodide ion. The upper part of VB states consists of the p(I) orbitals, and for slightly lower energy of the p (I_i) orbitals of the triiodide ion atoms. However, the CB minimum states came from the p(I_i) orbitals and for slightly larger energy of the p(Bi) and p(I) orbitals. These results are similar to those in the literature [29,30]. Then the intercalated triiodide orbitals play an important role and behave as a new CB minimum. This analysis also indicates that the inorganic Z2 and K2 anions ($[BiI_9]^{4-} = \left[(BiI_6)^{3-}\cdot I_3^-\right]$ and $[Bi_6I_{34}]^{12-} = 2\left\{[Bi_3I_{14}]^{5-} + I_3^-\right\}$ respectively) are mainly responsible of the electronic structure near the gap. In particular, the I_3^- ion is the cause of the Z2 and K2 gap reduction with respect to Z1 and K1.

Therefore, the influence of the anion states for all compounds on the absorption coefficients and conversion efficiency is decisive. This is like what happens with the organic lead iodine perovskites where the most important contributions to the states close to the band edges are

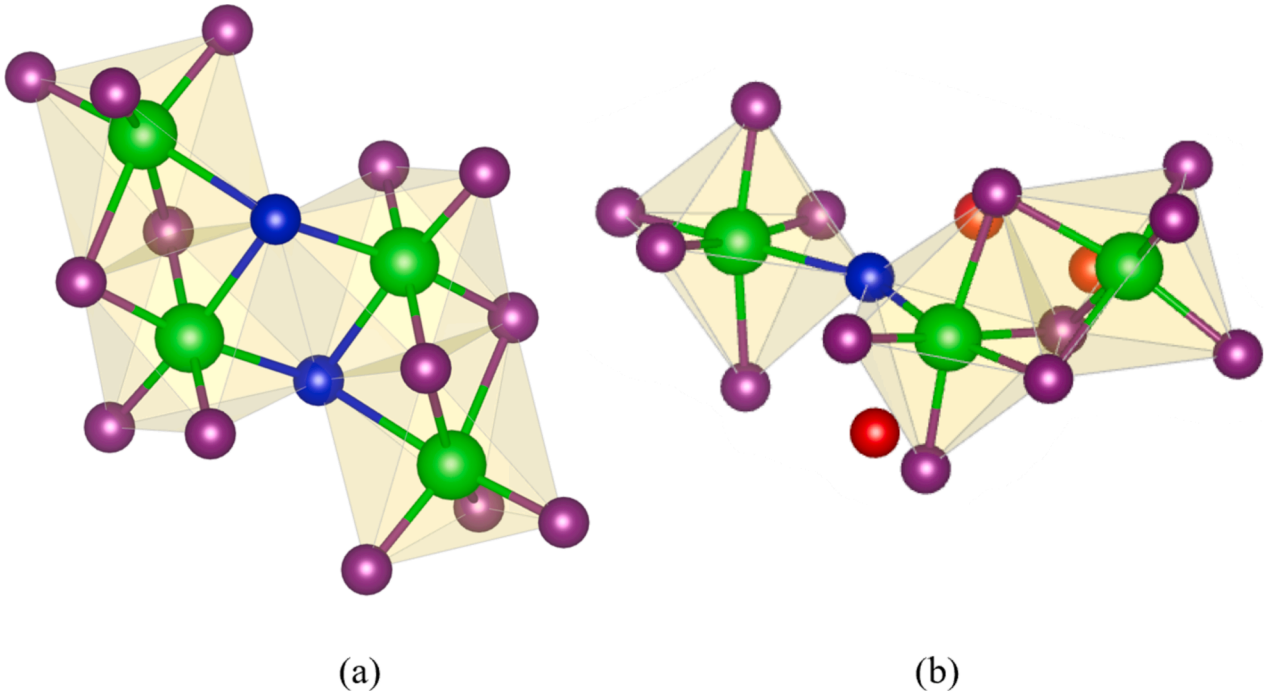

Fig. 2. Same legend as that in Fig. 1, but for the (a) K1 and (b) K2 compounds.

determined mainly by the inorganic anion states [10,27,28]. Later it will be justified that the Z1, Z2, K1 and K2 anion states also determine the optical properties.

In order to analyze and explore the correlation between absorption coefficients and crystalline structures, it is essential to consider the partitioning of absorption coefficients into contributions from various species. The more significant contributions are shown in Fig. 3 for the Z1 and Z2 compounds, and in Fig. 4 for the K1 and K2 compounds respectively. They correspond to the one- (intra-specie α_{A-A}) and two-specie contributions (inter-specie α_{A-B}). Note that intra-specie α_{A-A} contributions include intra-atomic (transitions between atomic states of the same atom A) and inter-atomic (transitions between states of atoms of the same specie A located at different sites) contributions. The inter-specie contributions α_{A-B} include only inter-atomic transitions. As mentioned above, in the Figures the iodine atoms have been divided into 3 groups: atoms bonded to a single Bi (I), bridge linker atoms bonded to two Bi simultaneously (I_l), and atoms not directly bonded to bismuth (I_i). The I_i atoms correspond to the triiodide ion I_3^- atoms.

For these compounds the combinations involving Bi, I, I_l, and I_i are the largest for the relevant energies of the solar radiation spectrum (lower than 3.5 eV). This highlights that the optical properties are predominantly influenced by the anionic part of the structure across all compounds. The contributions from cationic atoms are negligible compared to those from anionic atoms, particularly for energies near the optical gap. The significant contribution from organic cation atoms occurs at higher energies, similar to the behavior observed in organic lead iodine perovskite solar cells. For a specific type of anionic structure, the optical properties near the gap are minimally dependent on the organic cation [27,28], i.e. the most large contributions come from the anionic fragment.

The main anionic contributions correspond to transitions from VB to CB states. For all compounds the VB states consists of the p(I) orbitals and the CB states come mainly from the p(Bi) and p(I) states. Therefore, the Bi-Bi, I-I and Bi-I contributions (α_{Bi-Bi},α_{I-I}, and α_{Bi-I}) are among the most important. Additionally, for Z2 and K2 the p(I_i) orbitals contribute to the VB and CB edges. Therefore, the I_i-I_i contribution ($\alpha_{I_i-I_i}$) is very important for energies close to the optical gap. Other contributions such as iodine bridge linker atoms $\alpha_{I_l-I_l}$ are much less important. As a conclusion, the inclusion of triiodide ion results in a reduction of the energy optical gap approximating it to the optimum for maximum efficiency (~ 1.3 eV [39–41]). Thus, the potential of Z2 and K2 as absorbing materials for solar radiation increases.

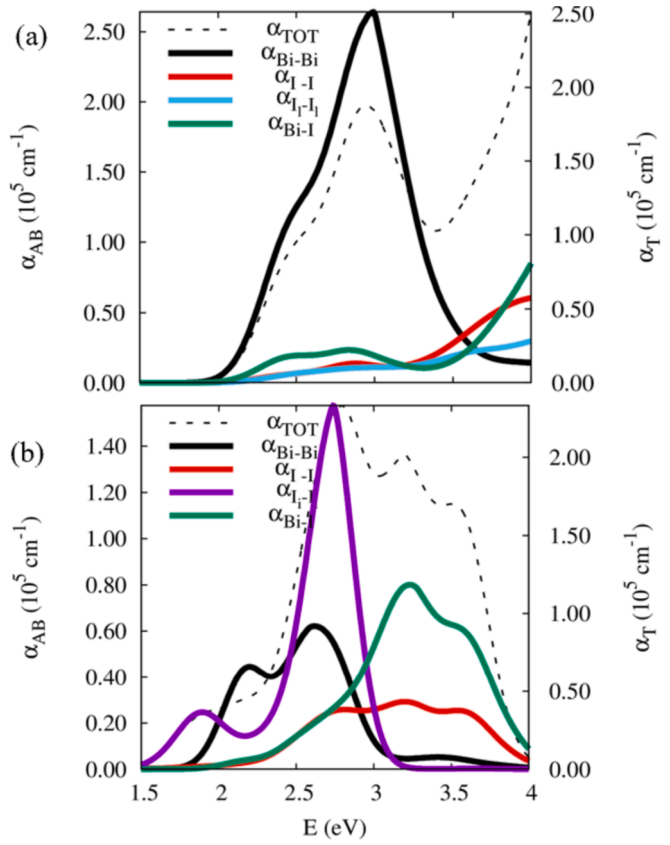

Fig. 3. Total absorption coefficient α_T (right y-axis) and absorption coefficient split into species contributions α_{AB} (left y-axis) as functions of the photon energy for the (a) Z1 and (b) Z2 compound anionic part.

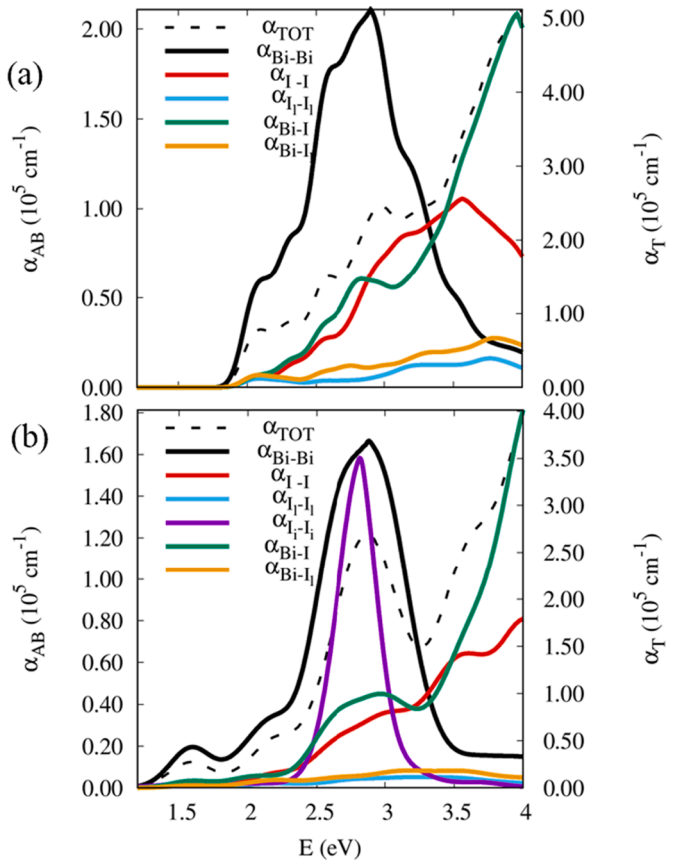

Fig. 4. Same legend as that in Fig. 3, but for the (a) K1 and (b) K2 compounds.

Z2 and K2 compounds present an absorption peak around 2.6 eV due to the $\alpha_{I_i-I_i}$ contributions. The $\alpha_{I_i-I_i}$ contributions for Z2 and K2 compounds are similar. However, the effect of the triiodide ion is more important for the Z2 compound (Fig. 3b), where the main contribution for this energy range is α_{Ii-Ii}, whereas for the K2 compound the $\alpha_{I_i-I_i}$ contributions are similar to the α_{Bi-Bi} contributions. This can be justified according to the structure. The Z2 and K2 inorganic anion structures are $[BiI_9]^{4-} = \left[(BiI_6)^{3-}\cdot I_3^-\right]$ (Fig. 1b) and $[Bi_3I_{17}]^{6-} = [Bi_3I_{14}]^{5-}\cdot I_3^-$ (Fig. 2b) respectively. The smallest I_i-I_i interatomic distance is comparable in both compounds (~2.9 Å). For this reason, the inter-atomic transitions involved in $\alpha_{I_i-I_i}$ are similar. The difference between Z2 and K2 is the inter-atomic transitions involved in α_{Bi-Bi}. These inter-atomic transitions implicate bicentric integrals, which decrease with the inter-atomic distance between the centers (atoms). The shortest Bi-Bi interatomic distances are 4.16 Å and 8.53 Å for compounds K2 and Z2 respectively. Therefore, the K2 α_{Bi-Bi} contribution is much larger than that of Z2 compound. In addition, there is another very important result that will be showed below when the efficiencies are analyzed. For the Z2 compound, and for energies from the optical gap to 3 eV, the most important contribution is from I_i-I_i. However, for the K2 compound the

Bi-Bi contribution is slightly more important than the I_i-I_i contribution.

Using the absorption coefficients previously obtained and the solar radiation spectrum, the efficiencies can be calculated [10]. The total efficiency η_T as a function of cell thickness w using the AM1.5G spectra [42] is shown on the right-hand y-axis in Fig. 5 for the Z1 and Z2 compounds, and Fig. 6 for the K1 and K2 compounds respectively. In the left-hand y-axis in Fig.s 5 and 6, the most important contributions of the many-body expansion of species contributions to the efficiencies are represented. These contributions are in agreement with that of the absorption coefficients in Fig.s 3 and 4. Comparing the total efficiency η_T of the Z2 and K2 compounds for larger w (~30.7 % and ~ 33.1 % respectively) with respect to the precursors Z1 and K1 (~23.2 % and ~ 25.0 % respectively), the triiodide ion insertion increases the efficiency η_T with respect to the precursor compounds ($\Delta\eta_T$~7.5 % and ~ 8.1 % for Z2 and K2 with respect to Z1 and K1 respectively).

The absorption of solar radiation depends on the thickness w and on the energy of the photons. The penetration depth of photons is inversely proportional to the absorption coefficient ($\alpha_T^{-1}(E)$). Therefore, for high energies where absorption coefficients are usually higher, the penetration depth is small. These high-energy photons are absorbed in a small thickness of the material. On the other hand, for energies close to the optical gap where the absorption coefficients are lower, the absorbing material needs to be very thick so that photons of these energies are absorbed. Therefore, the number of absorbed photons increases with thickness. For large thicknesses all photons in the solar spectrum are absorbed. Then, the total efficiency η_T and split efficiencies $\eta_{A\text{ - }B}$ increase with increasing thickness w. Above a certain thickness w, all the photons of the solar spectrum are absorbed and therefore the efficiency does not increase further. Fig.s 5 and 6 show that this fact occurs above thicknesses greater than ~ 1 μm, except for compound Z1 where the thickness is somewhat greater (~10 μm).

Similarly to what happened with the split absorption coefficients, the Bi-Bi, I-I and Bi-I contributions to η_T ($\eta_{Bi\text{ - }Bi}$,$\eta_{I\text{ - }I}$, and $\eta_{Bi\text{ - }I}$) are among the most important for all compounds. For Z2 and K2 the I_i-I_i contribution $\eta_{I_i\text{ - }I_i}$ is also very important. For the Z2 compound the main contribution is $\eta_{I_i\text{ - }I_i}$. However, for the K2 compound is $\eta_{Bi\text{ - }Bi}$. This is because the most important contribution to the Z2 absorption coefficient (Fig. 3b) in a wide range of energies from the optical gap energy to 3.0–3.5 eV corresponds to $\alpha_{I_i\text{ - }I_i}$, while in the case of the K2 corresponds to $\alpha_{Bi\text{ - }Bi}$(Fig. 4b).

This fact could lead to the assumption that the I_i-I_i contribution to the efficiency is not very large in the K2 compound. Nevertheless, according to the methodology section, the maximum efficiency depends on the absorption coefficients. The absorption threshold is the optical gap. A decrease in the optical gap therefore modifies the absorption coefficient, allowing more photons from the solar spectrum to be absorbed. Therefore, two types of contributions should be distinguished: (i) Explicit contribution for energies above the optical gap, shown in Figs. 5 and 6; (ii) implicit contribution, which is because of the optical gap reduction by the insertion of I_i atoms. For very thick solar cells, the reduction of the optical gap is the most significant factor. As mentioned above, the triiodide ion insertion leads to an efficiency increase of$\Delta\eta_T$ ~ 7.5 % for Z2 and ~ 8.1 % for K2 with respect to Z1 and K1 respectively.

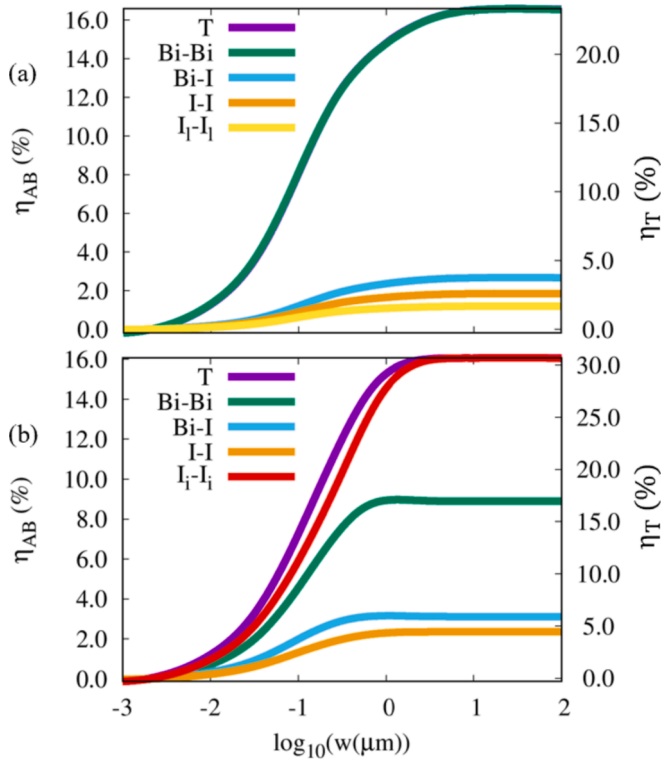

Fig. 5. Total efficiency η_T (right-hand y axis) and two-specie contributions η_{AB} (left-hand y axis) as a function of the cell thickness w decimal logarithm, using the AM1.5G spectra, for the (a) Z1 and (b) Z2 compounds.

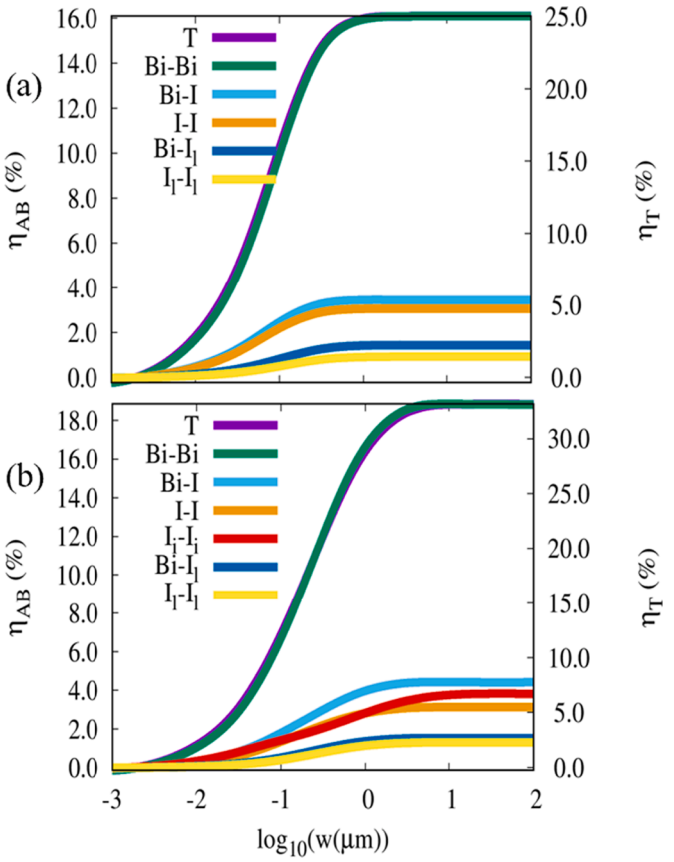

Fig. 6. Same legend as that in Fig. 5, but for the (a) K1 and (b) K2 compounds.

4. Conclusions

This study explores the potential of several Bi-based hybrid compounds, both with (Z2 and K2) and without (Z1 and K1) triiodide ions, as absorbers of solar radiation. The electronic and optical properties were determined using first principles. Additionally, the absorption coefficients were split into an exact many-species expansion. With the split absorption coefficients, and using the AM1.5G spectra, efficiencies as a function of cell thickness were calculated as an exact many-species expansion.

In these compounds, only the states of the anion atoms contribute to

both the VB and CB edge states. As a consequence, the contribution below 4 eV to the absorption coefficients is primarily due to the anion atoms. Furthermore, the inclusion of triiodide ions into the Z2 and K2 compounds leads to a reduction of the optical energy gap and an increase in absorption. It increases the potential of these compounds as photovoltaic absorbing materials.

Although the I_i-I_i contribution to the absorption coefficients and efficiencies is larger, the main difference between Z2 and K2 compounds is the Bi-Bi contribution. This is because the shortest Bi-Bi inter-atomic distances for Z2 are larger than for K2. This leads to the Bi-Bi contributions to the absorption coefficients and efficiencies for the K2 compound being more significant than for the Z2 compound, although in both cases there is an increment on the efficiency with respect to the precursor compounds Z1 and K1.

This work reinforces that halide anion incorporation can be a potential venue in making lead-free absorber materials competitive.

Author contributions

CTC contributed to every aspect of this work.

Ethical approval

Not applicable.

Data availability statement

All relevant data that support the findings of this study are presented in the manuscript. Source data can be available upon reasonable request from corresponding author.

CRediT authorship contribution statement

César Tablero-Crespo: Writing – review & editing, Writing – original draft, Visualization, Validation, Supervision, Software, Resources, Methodology, Investigation, Formal analysis, Data curation, Conceptualization.

Declaration of competing interest

The authors declare that they have no known competing financial interests or personal relationships that could have appeared to influence the work reported in this paper.

Acknowledgments

This work has been supported by the Project PVBOOSTER (Ref. PID2021-124193OB-C21) funded by the Ministerio de Ciencia e Innovación and co-funded with European Funds.

Data availability

Data will be made available on request.

References

[1] M.H. Ishraq, Md. Tarekuzzaman, J.K. Modak, S. Ahmad, Md. Rasheduzzaman, Y. Arafat, M.Z. Hasan, Investigating novel perovskites of lead-free flexible solar cell CH3NH3BiI3 and their photovoltaic performance with efficiency over 26%, Mater. Sci. Eng. B 308 (2024) 117622 https://doi.org/10.1016/j.mseb.2024.117622.
[2] X. Gu, L. Cao, S. Miao, X. Tao, Y. Zhao, S. Huang, A comprehensive review on preparation and humidity sensing applications of metal-halide perovskites, Mater. Sci. Eng. B 311 (2025) 117834, https://doi.org/10.1016/j.mseb.2024.117834.
[3] W. Zhang, X. Guo, Z. Cui, H. Yuan, Y. Li, W. Li, X. Li, J. Fang, Strategies for Improving Efficiency and Stability of Inverted Perovskite Solar Cells, Adv. Mater. 36 (2024) 2311025, https://doi.org/10.1002/adma.202311025.
[4] J. Huang, Z. Zhang, Y. Zhu, H. Yu, X. Li, Z. Liu, S. Kazim, Y. Hu, W. Yang, X. Ma, L. Dai, S. Ahmad, Y. Shen, M. Wang, Modulating Buried Interface to Achieve an Ultra-High Open Circuit Voltage in Triple Cation Perovskite Solar Cells, Adv. Energy Mater. 14 (2024) 2402469, https://doi.org/10.1002/aenm.202402469.
[5] T. Webb, S.J. Sweeney, W. Zhang, Device Architecture Engineering: Progress toward Next Generation Perovskite Solar Cells, Adv. Funct. Mater. 31 (2021) 2103121, https://doi.org/10.1002/adfm.202103121.
[6] Y. Bai, T. Wang, J. Yang, X. Pu, B. Xue, H. Chen, X. He, G. Feng, S. Jia, J. Yin, Q. Cao, X. Li, Enhancing efficiency and stability of inverted perovskite solar cells through synergistic suppression of multiple defects via poly(ionic liquid)-buried interface modification, J. Mater. Sci. Technol. 212 (2025) 281–288, https://doi.org/10.1016/j.jmst.2024.05.069.
[7] H. Chen, C. Liu, J. Xu, A. Maxwell, W. Zhou, Y. Yang, Q. Zhou, A.S.R. Bati, H. Wan, Z. Wang, L. Zeng, J. Wang, P. Serles, Y. Liu, S. Teale, Y. Liu, M.I. Saidaminov, M. Li, N. Rolston, S. Hoogland, T. Filleter, M.G. Kanatzidis, B. Chen, Z. Ning, E. H. Sargent, Improved charge extraction in inverted perovskite solar cells with dual-site-binding ligands, Science 384 (2024) 189–193, https://doi.org/10.1126/science.adm9474.
[8] Q. Chen, N.D. Marco, Y. (Michael) Yang, T.-B. Song, C.-C. Chen, H. Zhao, Z. Hong, H. Zhou, Y. Yang, Under the spotlight: The organic–inorganic hybrid halide perovskite for optoelectronic applications, Nano Today 10 (2015) 355–396, https://doi.org/10.1016/j.nantod.2015.04.009.
[9] P.P. Boix, K. Nonomura, N. Mathews, S.G. Mhaisalkar, Current progress and future perspectives for organic/inorganic perovskite solar cells, Mater. Today 17 (2014) 16–23, https://doi.org/10.1016/j.mattod.2013.12.002.
[10] C.T. Crespo, Contributions to Optical Properties and Efficiencies of Methyl–Ammonium Lead, Tin, and Germanium Iodide Perovskites, J. Phys. Chem. C 124 (2020) 12305–12310, https://doi.org/10.1021/acs.jpcc.0c02836.
[11] C. Tablero Crespo, Effect of Substitution of Pb for Mg on the Photovoltaic Properties of Methyl-Ammonium Lead Iodide Perovskites, Adv. Theory Simul. 5 (2022) 2100509, https://doi.org/10.1002/adts.202100509.
[12] C. Lu, J. Zhang, D. Hou, X. Gan, H. Sun, Z. Zeng, R. Chen, H. Tian, Q. Xiong, Y. Zhang, Y. Li, Y. Zhu, Calcium doped MAPbI3 with better energy state alignment in perovskite solar cells, Appl. Phys. Lett. 112 (2018) 193901, https://doi.org/10.1063/1.5020840.
[13] D. Pérez-del-Rey, D. Forgács, E.M. Hutter, T.J. Savenije, D. Nordlund, P. Schulz, J. J. Berry, M. Sessolo, H.J. Bolink, Strontium Insertion in Methylammonium Lead Iodide: Long Charge Carrier Lifetime and High Fill-Factor Solar Cells, Adv. Mater. 28 (2016) 9839–9845, https://doi.org/10.1002/adma.201603016.
[14] H. Zhang, M. Shang, X. Zheng, Z. Zeng, R. Chen, Y. Zhang, J. Zhang, Y. Zhu, Ba2+ Doped CH3NH3PbI3 to Tune the Energy State and Improve the Performance of Perovskite Solar Cells, Electrochim. Acta 254 (2017) 165–171, https://doi.org/10.1016/j.electacta.2017.09.091.
[15] M.R. Filip, F. Giustino, Computational Screening of Homovalent Lead Substitution in Organic–Inorganic Halide Perovskites, J. Phys. Chem. C 120 (2016) 166–173, https://doi.org/10.1021/acs.jpcc.5b11845.
[16] X. Ma, R. Luo, X. Li, H. Yu, J. Huang, W. Yang, H. Shi, Y. Shen, M. Wang, Migration and evolution of iodine in perovskite solar cells, Mater. Today Phys. 50 (2025) 101616, https://doi.org/10.1016/j.mtphys.2024.101616.
[17] X. Lu, K. Sun, Y. Wang, C. Liu, Y. Meng, X. Lang, C. Xiao, R. Tian, Z. Song, Z. Zhu, M. Yang, Y. Bai, Z. Ge, Dynamic Reversible Oxidation-Reduction of Iodide Ions for Operationally Stable Perovskite Solar Cells under ISOS-L-3 Protocol, Adv. Mater. 36 (2024) 2400852, https://doi.org/10.1002/adma.202400852.
[18] L. Yu, R.S. Kokenyesi, D.A. Keszler, A. Zunger, Inverse Design of High Absorption Thin-Film Photovoltaic Materials, Adv. Energy Mater. 3 (2013) 43–48, https://doi.org/10.1002/aenm.201200538.
[19] A. Khan, H. Wen, S. Iqbal, M. Rehman, M. Shah, M. Raheel, F.A. Khan, R. Khan, R. A. Althobiti, E. Alzahrani, A.-E. Farouk, F.F. Al-Fawzan, E.B. Elkaeed, A bismuth-based (III) hybrid perovskite as a highly air-stable, potential absorber with photoconductive response, Opt. Mater. 143 (2023) 114228, https://doi.org/10.1016/j.optmat.2023.114228.
[20] X. Hu, Y. Zhu, J. Wang, G. Zheng, D. Yao, B. Lin, N. Tian, B. Zhou, F. Long, Stable organic-inorganic hybrid bismuth-halide: Exploration of crystal-structural, morphological, thermal, spectroscopic and optoelectronic properties, J. Mol. Struct. 1264 (2022) 133102, https://doi.org/10.1016/j.molstruc.2022.133102.
[21] Y. Zhang, M. Ghasemi, X. Wen, M. Lee, X. Liu, Y. Jiao, P.V. Bernhardt, E. Han, T. Lin, B.W. Zhang, K. Xu, S.-M. Lee, J.S. Yun, J.-H. Yun, L. Wang, Reversible structural transformation of metastable lead-free organic–inorganic hybrid bismuth halide single crystals, J. Mater. Chem. A 12 (2024) 29152–29164, https://doi.org/10.1039/D4TA04715J.
[22] A.A. Babaryk, Y. Pérez, M. Martínez, M.E.G. Mosquera, M.H. Zehender, S. A. Svatek, E. Antolín, P. Horcajada, Reversible dehydration–hydration process in stable bismuth-based hybrid perovskites, J. Mater. Chem. C 9 (2021) 11358–11367, https://doi.org/10.1039/D1TC01730F.
[23] S.A. Adonin, A.N. Usoltsev, A.S. Novikov, B.A. Kolesov, V.P. Fedin, M.N. Sokolov, One- and Two-Dimensional Iodine-Rich Iodobismuthate(III) Complexes: Structure, Optical Properties, and Features of Halogen Bonding in the Solid State, Inorg. Chem. 59 (2020) 3290–3296, https://doi.org/10.1021/acs.inorgchem.9b03734.
[24] T. Nie, Z. Fang, X. Ren, Y. Duan, S. (Frank) Liu, Recent Advances in Wide-Bandgap Organic–Inorganic Halide Perovskite Solar Cells and Tandem Application, Nano-Micro Lett. 15 (2023) 70, https://doi.org/10.1007/s40820-023-01040-6.
[25] P. Priyadarshini, S. Senapati, R. Naik, Lead-free organic inorganic hybrid halide perovskites: An emerging candidate for bifunctional applications, Renew. Sustain. Energy Rev. 186 (2023) 113649, https://doi.org/10.1016/j.rser.2023.113649.
[26] T. Pinky, D.A. Popy, Z. Zhang, J. Jiang, R. Pachter, B. Saparov, Synthesis and Characterization of New Hybrid Organic–Inorganic Metal Halides [(CH3)3SO] M2I3 (M = Cu and Ag), Inorg. Chem. 63 (2024) 2174–2184, https://doi.org/10.1021/acs.inorgchem.3c04119.

[27] C.T. Crespo, Effect Of the organic cation on the optical properties of lead iodine perovskites, Sol. Energy Mater. Sol. Cells 200 (2019) 110022, https://doi.org/10.1016/j.solmat.2019.110022.
[28] C.T. Crespo, The effect of the halide anion on the optical properties of lead halide perovskites, Sol. Energy Mater. Sol. Cells 195 (2019) 269–273, https://doi.org/10.1016/j.solmat.2019.03.023.
[29] W. Zhang, X. Liu, L. Li, Z. Sun, S. Han, Z. Wu, J. Luo, Triiodide-Induced Band-Edge Reconstruction of a Lead-Free Perovskite-Derivative Hybrid for Strong Light Absorption, Chem. Mater. 30 (2018) 4081–4088, https://doi.org/10.1021/acs.chemmater.8b01200.
[30] B. Kou, W. Zhang, C. Ji, Z. Wu, S. Zhang, X. Liu, J. Luo, Tunable optical absorption in lead-free perovskite-like hybrids by iodide management, Chem Commun 55 (2019) 14174–14177, https://doi.org/10.1039/C9CC05365D.
[31] W. Kohn, L.J. Sham, Self-Consistent Equations Including Exchange and Correlation Effects, PhysRev 140 (1965) A1133–A1138, https://doi.org/10.1103/PhysRev.140.A1133.
[32] J.M. Soler, E. Artacho, J.D. Gale, A. García, J. Junquera, P. Ordejón, Daniel Sánchez-Portal, The SIESTA method for ab initio order- N materials simulation, J. Phys. Condens. Matter 14 (2002) 2745.
[33] J.P. Perdew, K. Burke, M. Ernzerhof, Generalized Gradient Approximation Made Simple, PhysRevLett 77 (1996) 3865–3868, https://doi.org/10.1103/PhysRevLett.77.3865.
[34] N. Troullier, J.L. Martins, Efficient pseudopotentials for plane-wave calculations, PhysRevB 43 (1991) 1993–2006, https://doi.org/10.1103/PhysRevB.43.1993.
[35] L. Kleinman, D.M. Bylander, Efficacious Form for Model Pseudopotentials, PhysRevLett 48 (1982) 1425–1428, https://doi.org/10.1103/PhysRevLett.48.1425.
[36] D.M. Bylander, L. Kleinman, 4f resonances with norm-conserving pseudopotentials, PhysRevB 41 (1990) 907–912, https://doi.org/10.1103/PhysRevB.41.907.
[37] O.F. Sankey, D.J. Niklewski, Ab initio multicenter tight-binding model for molecular-dynamics simulations and other applications in covalent systems, Phys. Rev. B 40 (1989) 3979–3995.
[38] G.F. Bassani, Electronic states and optical transitions in solids, Pergamon Press, Oxford, New York, 1975.
[39] A. Luque, A. Martí, Theoretical Limits of Photovoltaic Conversion, in Handbook of Photovoltaic Science and Engineering, Edited by A. Luque and S. Hegedus, John Wiley & Sons Ltd, 2003.
[40] P. Würfel, Physics of Solar Cells, WILEY-VCH Verlag GmbH & Co, KGaA, From Principles to New Concepts, 2005.
[41] M.A. Green, Third Generation Photovoltaics, Springer-Verlag, Berlin Heidelberg, Advanced Solar Energy Conversion, 2003.
[42] http://rredc.nrel.gov/solar/spectra/am1.5/ASTMG173/ASTMG173.html, n.d.